Cancer Management and Research

Elevate Series

Open Access Full Text Article

ORIGINAL RESEARCH

Development and Validation of a Prognostic Nomogram for Endometrial Cancer Based on Systemic Immune-Inflammation Index and Key Clinicopathological Features

Jialu Lu[1,2], Ziyi Lin[1,2], Yu Tian[3], Minghui Zhou[2], Yanqin Ji[1,2]

[1]The First Clinical Medical College, Guangdong Medical University, Zhanjiang, Guangdong, People's Republic of China; [2]Department of Gynecological Oncology, Huizhou Central People's Hospital, Huizhou, Guangdong, People's Republic of China; [3]Research Center, Huizhou Central People's Hospital, Guangdong Medical University, Huizhou, Guangdong, People's Republic of China

Correspondence: Yanqin Ji; Minghui Zhou, Email yanqinji8899@163.com; ppa666@163.com

Objective: This study aimed to develop and validate a prognostic nomogram integrating systemic immune-inflammatory index (SII) and key clinicopathological features for predicting 2-, 3-, and 5-year overall survival (OS, primary surgery to all-cause death) in patients with Endometrial Cancer (EC), subgrouped into Survivors or Non-survivors, so as to address the unmet need for low-cost, dynamic risk stratification tools in EC precision medicine.

Methods: A retrospective cohort of 341 patients with EC (per WHO 2020 criteria) from January 2015 to January 2023 was stratified randomly into training (60%, n=205) and validation (40%, n=136) sets (stratification factors: age). Independent prognostic factors were identified through LASSO and multivariate Cox regression analyses. A nomogram was constructed and evaluated using ROC curves, calibration plots, and decision curve analysis (DCA). Key indicators included pathological differentiation grade, lymphovascular space invasion (LVSI), and systemic immune-inflammatory index (SII).

Results: Four independent predictors were identified: age (HR = 1.039, 95% CI: 0.994–1.086, $P = 0.002$), pathological differentiation grade (HR = 0.384, 95% CI: 0.188–0.786, $P = 0.001$), LVSI (HR = 4.208, 95% CI: 1.523–11.625, $P = 0.001$), and SII (HR = 1.001, 95% CI: 1.001–1.002, $P < 0.001$). The nomogram demonstrated excellent discrimination, with AUCs of 0.881, 0.883, and 0.874 for 2-, 3-, and 5-year OS in the training cohort, and 0.870, 0.834, and 0.838 in the validation cohort.

Conclusion: This study successfully developed and validated a prognostic model for EC based on SII and pathological differentiation. The model significantly outperformed traditional clinical parameters and may serve as a valuable tool for early risk stratification and individualized management in clinical practice.

Keywords: endometrial cancer, prognosis, nomogram, systemic immune-inflammation index, overall survival, predictive model

Introduction

Endometrial cancer (EC) is the most common gynecological malignancy in developed countries and represents a significant public health burden globally. In 2020, an estimated 417,000 new cases were diagnosed worldwide, accounting for 4.5% of all cancers in women.[1] Although the majority of patients are diagnosed at an early stage with favorable outcomes, a substantial subset experiences recurrence and poor survival, highlighting the need for improved prognostic stratification.[2]

EC is a heterogeneous disease influenced by hormonal, genetic, and environmental factors. Traditional prognostic assessment relies on the International Federation of Gynecology and Obstetrics (FIGO) staging, histological grade, and lymph node status.[3] However, these parameters alone often fail to capture the dynamic interplay between tumor biology and host immune response, which plays a critical role in disease progression and treatment resistance.[4]

In recent years, systemic inflammatory markers derived from routine blood tests, such as the neutrophil-to-lymphocyte ratio (NLR), platelet-to-lymphocyte ratio (PLR), and systemic immune-inflammation index (SII), have emerged as promising prognostic indicators across various cancers.[5–7] These indices reflect the balance between pro-

https://doi.org/10.2147/CMAR.S572098
Received: 25 October 2025
Accepted: 30 January 2026
Published: 11 February 2026

tumor inflammation and anti-tumor immunity, offering insights into the tumor microenvironment and patient immune status. Among them, SII—calculated as platelet count × neutrophil count/lymphocyte count—integrates three key cellular components and has shown superior prognostic value in several malignancies.[8,9]

Despite growing evidence, few studies have incorporated SII into a comprehensive prognostic model for EC that also integrates established clinicopathological variables. Existing prognostic tools often lack accessibility, rely on costly molecular testing, or fail to account for systemic inflammation.[10,11] Therefore, there is a clear need for a readily applicable, cost-effective, and biologically informative prognostic model that can be implemented in routine clinical practice.

This study aimed to develop and validate a prognostic nomogram for EC based on SII and key clinicopathological features. We hypothesize that integrating inflammatory indices with traditional pathological factors will enhance prognostic accuracy and provide a practical tool for individualized patient management.

Method

Study Design and Patient Cohort

This was a single-center, retrospective cohort study conducted at Huizhou Central People's Hospital. We reviewed the records of 448 consecutive patients diagnosed with EC who underwent primary surgical treatment between January 2015 and January 2023. The study was approved by the hospital's Ethics Committee (No. kyll2025081). Due to the retrospective nature, the requirement for informed consent was waived. All enrolled patients were diagnosed in accordance with the diagnostic criteria for EC specified in the WHO Classification of Tumours of the Female Reproductive System (2020 Edition), confirmed by hysteroscopic biopsy combined with postoperative paraffin section pathological examination. Pathological sections were independently reviewed by two senior gynecological pathologists using a double-blind method; in case of diagnostic discrepancy, consensus was reached through a departmental pathology conference.

Inclusion and Exclusion Criteria

Inclusion criteria were: (1) histopathological confirmation of EC post-surgery; (2) Underwent total hysterectomy combined with bilateral salpingo-oophorectomy or staging surgery (ovarian preservation permitted in select young patients after detailed evaluation); (3) availability of preoperative complete blood count (CBC) drawn within 24–72 hours before surgery, with patients fasting and free from acute infection or stress; (4) complete clinical, surgical, pathological, and follow-up data. Exclusion criteria included: (1) other primary malignancies; (2) preoperative anticancer therapy; (3) active autoimmune or chronic inflammatory diseases; (4) significant hepatic/renal dysfunction; (5) incomplete records. After screening, 341 patients were enrolled.

Data Collection and Definitions

Data were extracted by two independent researchers. Clinical variables included age, BMI, comorbidities (hypertension, diabetes, coronary heart disease), and menstrual/reproductive history. Preoperative CBC was used to calculate inflammatory indices: NLR (neutrophils/lymphocytes), PLR (platelets/lymphocytes), LMR (lymphocytes/monocytes), and SII (platelets × neutrophils/lymphocytes). Pathological variables were obtained from final reports: FIGO stage (2009), histological type, tumor grade (G1/well, G2/moderate, G3/poor), myometrial invasion depth (<50% vs ≥50%), lymphovascular space invasion (LVSI), lymph node metastasis, and Ki-67 index. The primary endpoint was overall survival (OS), defined as the time from surgery to death from any cause. Patients alive at last follow-up (Dec 31, 2023) were censored.

Statistical Analysis

Statistical analyses were performed using SPSS 26.0 and R 4.4.1. The cohort was divided into a training set (60%, n=205) for model development and a validation set (40%, n=136) for internal validation using the method of age-stratified random sampling. The median age of the enrolled patients was 53 years, based on which the patients were stratified into two subgroups: ≤ 53 years and > 53 years. Within each stratum, random allocation was performed at a 6:4 ratio using the random number table method, so as to avoid model verification bias caused by age confounding and ensure the comparability of baseline risks between the two sets. The training and validation sets were partitioned at a 6:4 ratio to moderately expand the

validation set size for more robust evaluation of model generalization ability, while ensuring sufficient training set samples to support model development.[12] Continuous variables were compared using t-tests or Mann–Whitney *U*-tests; categorical variables using chi-square or Fisher's exact tests. In the training set, univariate Cox regression was performed for initial screening (P<0.10). To prevent overfitting and select the most relevant predictors, Least Absolute Shrinkage and Selection Operator (LASSO) regression with 10-fold cross-validation was applied. Variables with non-zero coefficients from LASSO were entered into a multivariate Cox proportional hazards model (backward stepwise, P<0.05 for retention). Based on the final Cox model, a prognostic nomogram was constructed. Model performance was evaluated by: (1) Discrimination: using time-dependent receiver operating characteristic (ROC) curves and calculating the area under the curve (AUC) at 2, 3, and 5 years. (2) Calibration: using calibration plots comparing predicted and observed (Kaplan-Meier) survival probabilities. (3) Clinical utility: using decision curve analysis (DCA) to assess net benefit across a range of threshold probabilities. A two-tailed P-value <0.05 was considered significant.

Results

Patient Characteristics and Survival Outcomes

The final cohort comprised 341 EC patients with a median age of 53 years (IQR: 48–58). Most had endometrioid histology (89.7%) and early-stage (FIGO I–II) disease (94.7%). After a median follow-up of 52 months (IQR: 36–68), 42 patients (12.3%) had died. Comparative analysis between survivors (n=299) and non-survivors (n=42) revealed significant differences in several key parameters (Table 1). Non-survivors were significantly older (median 58 vs 53 years, P=0.03), had a higher proportion of poorly differentiated tumors (52.4% vs 12.7%, P<0.001), more frequent lymphatic metastasis (19% vs 3.3%, P<0.001) and vascular tumor thrombus invasion (45.2% vs 17.4%, P<0.001). Regarding inflammatory markers, non-survivors had significantly higher median NLR (2.5 vs 2.0, P=0.048) and SII (752.2 vs 591.8, P=0.017). The training (n=205) and validation (n=136) sets were well-balanced for most baseline characteristics, with no significant differences except for lymph node metastasis (P=0.039) and depth of invasion (P=0.005) (Table 2).

Table 1 Summary of Clinically, Laboratory, and Pathological Parameters with Statistically Significant Differences Among the Study Groups (*P* < 0.05)

	Survivor Group	Non-Survivors Group	Total	*P* value
Total	299	42	341	
Age				0.03
Median (IQR[1])	53(47.5,57)	58(49,65)	53(48,58)	
American Society of Anesthesiologists physical status classification (ASA)				0.931
Level 1 group	39(13)	5(11.9)	44(12.9)	
Level 2 group	255(85.3)	36(85.7)	291(85.3)	
Level 3 group	5(1.7)	1(2.4)	6(1.8)	
Duration of surgery (hours)				0.195
Median (IQR)	3(1.8,4.2)	3.5(1.9,4.7)	3(1.8,4.2)	
Hypertension				0.464
Absent	229(76.6)	30(71.4)	259(76)	
Present	70(23.4)	12(28.6)	82(24)	
Diabetes				0.595
Absent	262(87.6)	38(90.5)	300(88)	
Present	37(12.4)	4(9.5)	41(12)	
Coronary heart disease				0.41
Absent	296(99)	41(97.6)	337(98.8)	
Present	3(1)	1(2.4)	4(1.2)	
Age at menarche				0.606
Median (IQR)	15(13,16)	15(13,16)	15(13,16)	

(*Continued*)

https://doi.org/10.2147/CMAR.S572098

Table 1 (Continued).

	Survivor Group	Non-Survivors Group	Total	*P* value
Regularity of menstruation				1
Absent	13(4.3)	1(2.4)	14(4.1)	
Present	286(95.7)	41(97.6)	327(95.9)	
Menopause				0.055
Absent	154(51.5)	15(35.7)	169(49.6)	
Present	145(48.5)	27(64.3)	172(50.4)	
Maternal history				0.382
Absent	13(4.3)	0(0)	13(3.8)	
Present	286(95.7)	42(100)	328(96.2)	
Height				0.715
Median (IQR)	156(153,159)	156(152,159)	156(153,159)	
Weight				0.719
Median (IQR)	59(53,65)	57.5(52.1,63.2)	59(53,65)	
Hemoglobin				0.645
Median (IQR)	127(111.5,135)	123.5(113,135.2)	127(112,135)	
Alanine Aminotransferase (ALT)				0.431
Median(IQR)	16(12,21)	17.5(12,23)	16(12,22)	
Aspartate Aminotransferase (AST)				0.138
Median (IQR)	18(14.7,21)	19(15,24)	18(15,21)	
Anion Gap (AG)				0.67
Median (IQR)	11.3(8.8,14)	10.8(8.9,14)	11.1(8.8,14)	
Creatinine				0.628
Median (IQR)	63(56,72)	63(55.2,76.8)	63(56,72)	
Blood Urea Nitrogen (BUN)				0.252
Median (IQR)	4.5(3.7,5.3)	4.8(3.9,5.9)	4.6(3.7,5.3)	
Total cholesterol				0.193
Median (IQR)	4.9(4.1,5.7)	5.2(4.5,6)	4.9(4.2,5.7)	
Glucose				0.734
Median (IQR)	5.4(5,6)	5.4(5.1,6.3)	5.4(5,6.1)	
Cancer Antigen 125 (CA125)				0.074
Median (IQR)	19.2(12.7,30)	21(16.1,40.1)	19.4(13,31.7)	
Cancer Antigen 199 (CA199)				0.295
Median (IQR)	14.9(8.2,26.7)	16.7(9.7,34.4)	15.2(8.3,27)	
Lactate Dehydrogenase (LDH)				0.73
Median (IQR)	194(165,229.5)	193.5(178,223)	194(168,229)	
Pathological differentiation degree				<0.001
Poorly differentiated (Grade 3)	38(12.7)	22(52.4)	60(17.6)	
Moderately differentiated (Grade 2)	198(66.2)	12(28.6)	210(61.6)	
Well differentiated (Grade 1)	63(21.1)	8(19)	71(20.8)	
Grade				0.013
1	272(91)	34(81)	306(89.7)	
2	14(4.7)	1(2.4)	15(4.4)	
3	13(4.3)	7(16.7)	20(5.9)	

(*Continued*)

Table 1 (Continued).

	Survivor Group	Non-Survivors Group	Total	*P* value
Lymphatic Metastasis				<0.001
Absent	289(96.7)	34(81)	323(94.7)	
Present	10(3.3)	8(19)	18(5.3)	
Vascular invasion				<0.001
Absent	247(82.6)	23(54.8)	270(79.2)	
Present	52(17.4)	19(45.2)	71(20.8)	
Invasion Depth				0.094
Shallow	246(82.3)	30(71.4)	276(80.9)	
Deep	53(17.7)	12(28.6)	65(19.1)	
Ki-67				0.032
Median (IQR)	40(20,70)	50(30,70)	40(20,70)	
NLR				0.048
Median (IQR)	2(1.6,2.8)	2.5(1.7,3.6)	2(1.6,2.8)	
PLR				0.404
Median (IQR)	141.9(106,178.9)	144.1(112.6,220.2)	141.9(106.6,183.5)	
LMR				0.445
Median (IQR)	4.4(3.4,5.6)	4.2(3,5.6)	4.4(3.4,5.6)	
SII				0.017
Median (IQR)	591.8(429.9,850.9)	752.2(463.7,1250.2)	605.8(430.2,879.9)	

Notes: [1]Interquartile Range.

Table 2 Comparison of Baseline Characteristics Between the Training Cohort and the Validation Cohort

	Test	Train	Total	*P* value
Total	136	205	341	
Age				0.997
Mean (SD)	53.1(8.4)	53.1(8.3)	53.1(8.3)	
ASA				0.445
Level 1 group	21(15.4)	23(11.2)	44(12.9)	
Level 2 group	112(82.4)	179(87.3)	291(85.3)	
Level 3 group	3(2.2)	3(1.5)	6(1.8)	
Duration of surgery (hours)				0.198
Median (IQR)	2.7(1.7,4.4)	3.2(1.8,4.2)	3(1.8,4.2)	
Hypertension				0.939
Absent	103(75.7)	156(76.1)	259(76)	
Present	33(24.3)	49(23.9)	82(24)	
Diabetes				0.905
Absent	120(88.2)	180(87.8)	300(88)	
Present	16(11.8)	25(12.2)	41(12)	
Coronary heart disease				0.652
Absent	134(98.5)	203(99)	337(98.8)	
Present	2(1.5)	2(1)	4(1.2)	
Age at menarche				0.955
Median (IQR)	15(13,16)	15(13,16)	15(13,16)	

(*Continued*)

https://doi.org/10.2147/CMAR.S572098

Table 2 (Continued).

	Test	Train	Total	*P* value
Regularity of menstruation				0.745
Absent	5(3.7)	9(4.4)	14(4.1)	
Present	131(96.3)	196(95.6)	327(95.9)	
Menopause				0.452
Absent	64(47.1)	105(51.2)	169(49.6)	
Present	72(52.9)	100(48.8)	172(50.4)	
Maternal history				0.638
Absent	6(4.4)	7(3.4)	13(3.8)	
Present	130(95.6)	198(96.6)	328(96.2)	
Height				0.985
Median (IQR)	157(153,159)	156(153,159)	156(153,159)	
Weight				0.208
Median (IQR)	58.8(52.4,64)	60(53,65)	59(53,65)	
Hemoglobin				0.767
Median (IQR)	128(112,135.2)	127(111,135)	127(112,135)	
ALT				0.149
Median (IQR)	16(13,22)	15.9(11,21.3)	16(12,22)	
AST				0.156
Median (IQR)	19(16,22)	17.7(14,21)	18(15,21)	
AG				0.511
Median (IQR)	11(9,13.7)	11.5(8.8,14)	11.1(8.8,14)	
Creatinine				0.061
Median (IQR)	61.5(55.8,67.2)	65(57,74)	63(56,72)	
BUN				0.659
Median (IQR)	4.5(3.7,5.3)	4.6(3.7,5.3)	4.6(3.7,5.3)	
Total cholesterol				0.671
Median (IQR)	5(4.1,5.7)	4.9(4.4,5.9)	4.9(4.2,5.7)	
Glucose				0.985
Median (IQR)	5.4(5,6.1)	5.5(4.9,6)	5.4(5,6.1)	
CA125				0.754
Median (IQR)	19.5(13.8,30.1)	19.2(12.7,32.6)	19.4(13,31.7)	
CA199				0.493
Median (IQR)	15.7(10.1,29.6)	15.1(8.1,25.6)	15.2(8.3,27)	
LDH				0.747
Median (IQR)	195(171.8,229)	193(168,229)	194(168,229)	
Pathological differentiation degree				0.166
Poorly differentiated (Grade 3)	28(20.6)	32(15.6)	60(17.6)	
Moderately differentiated (Grade 2)	86(63.2)	124(60.5)	210(61.6)	
Well differentiated (Grade 1)	22(16.2)	49(23.9)	71(20.8)	

(*Continued*)

Table 2 (Continued).

	Test	Train	Total	*P* value
Grade				0.573
1	123(90.4)	183(89.3)	306(89.7)	
2	7(5.1)	8(3.9)	15(4.4)	
3	6(4.4)	14(6.8)	20(5.9)	
Lymphatic Metastasis				0.039
Absent	133(97.8)	190(92.7)	323(94.7)	
Present	3(2.2)	15(7.3)	18(5.3)	
Vascular invasion				0.316
Absent	104(76.5)	166(81)	270(79.2)	
Present	32(23.5)	39(19)	71(20.8)	
Invasion Depth				0.005
Shallow	120(88.2)	156(76.1)	276(80.9)	
Deep	16(11.8)	49(23.9)	65(19.1)	
Ki-67				0.187
Median (IQR)	40(20,60)	40(20,70)	40(20,70)	
NLR				0.277
Median (IQR)	2.1(1.6,2.9)	2(1.6,2.8)	2(1.6,2.8)	
PLR				0.759
Median (IQR)	141.7(111.6,184.1)	142.9(106.2,175.5)	141.9(106.6,183.5)	
LMR				0.35
Median (IQR)	4.3(3.3,5.5)	4.4(3.5,5.6)	4.4(3.4,5.6)	
SII				0.501
Median (IQR)	605.3 (418.1,876.2)	609.5 (450.4,883.5)	605.8(430.2,879.9)	
Follow-up Outcome				0.207
Alive	123(90.4)	176(85.9)	299(87.7)	
Dead	13(9.6)	29(14.1)	42(12.3)	

Predictor Selection and Multivariate Cox Regression Analysis

In the training set, univariate Cox analysis identified several potential predictors for OS. Subsequently, LASSO regression (Figures 1A and B) was employed for variable selection, which adopted 10-fold cross-validation to determine the optimal penalty parameter λ for minimizing partial likelihood deviance, further reducing the risk of model overfitting; this approach narrowed down 12 candidate variables to a more parsimonious set. These selected variables were then entered into the multivariate Cox proportional hazards model. The final model identified four independent prognostic factors for OS (Table 3): age (HR = 1.039, 95% CI: 0.994–1.086, $P = 0.002$), pathological differentiation grade (with poorer differentiation associated with worse survival; HR = 0.384, 95% CI: 0.188–0.786, $P = 0.001$), lymphovascular space invasion (LVSI; HR = 4.208, 95% CI: 1.523–11.625, $P = 0.001$), and systemic immune-inflammation index (SII; HR = 1.001, 95% CI: 1.001–1.002, $P < 0.001$). Notably, NLR did not retain independent significance in the final multivariate model ($P = 0.0502$).

Nomogram Construction and Performance Validation

Based on the four independent predictors, a prognostic nomogram was constructed to provide individualized estimates of 2-, 3-, and 5-year overall survival probabilities (Figure 2). Each predictor is assigned a score on the "Points" scale; the sum of these scores corresponds to a total point value, which is then projected downward to the survival probability axes. The model demonstrated strong discriminatory ability. In the training cohort, the AUCs for predicting 2-, 3-, and 5-year

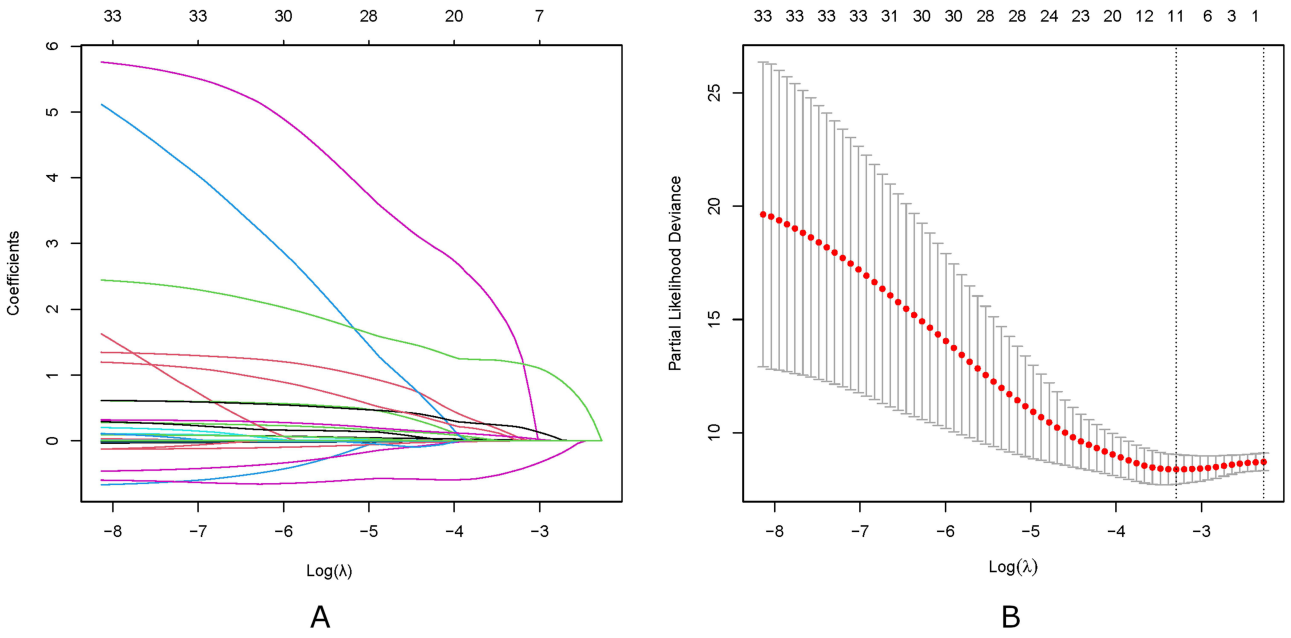

Figure 1 LASSO Regression for Variable Selection in Prognostic Modeling. (**A**) Log(λ)-Regularized Shrinkage Curves of Candidate Variables' Coefficients (**B**) Trend Plot of the Relationship between Log(λ) and Binomial Deviance (Including 95% Confidence Intervals). (**A**) illustrates the relationship between the logarithmic value of λ (Logλ) and component coefficients, which are plotted against the logarithmically transformed regularization parameter (log(λ)). Curves in distinct colors correspond to the variation tendencies of coefficients for different components as a function of the logarithmic value of λ. (**B**) illustrates the relationship between the logarithm of λ (Log(λ)) and the binomial deviance, specifically depicting the process of selecting the optimal tuning parameter via 10-fold cross-validation. The red curve distinctly delineates the variation trend between the two variables, with the 95% confidence interval band (gray shaded region) and vertical dashed lines corresponding to two critical u values concomitantly annotated in the figure.

OS were 0.881 (95% CI: 0.739–1.000), 0.883 (95% CI: 0.799–0.968), and 0.874 (95% CI: 0.771–0.978), respectively (Figure 3A). In the validation cohort, the model maintained robust performance with corresponding AUCs of 0.870 (95% CI: 0.748–0.991), 0.834 (95% CI: 0.723–0.945), and 0.838 (95% CI: 0.696–0.980) (Figure 3B).

Calibration plots for both the training and validation sets showed good agreement between the nomogram-predicted survival probabilities and the actual observed outcomes (Kaplan-Meier estimates) at 3 and 5 years, with the calibration curves closely aligning with the ideal 45-degree line (Figures 4A and B). Decision curve analysis (DCA) further confirmed the clinical utility of the nomogram. The DCA curves (Figures 5A–F) demonstrated that across a wide range of threshold probabilities (risk thresholds where a clinician would consider intervention), the use of this nomogram to guide decisions provided a higher net benefit compared to the strategies of "treating all patients" or "treating none," in both the training and validation cohorts at 2, 3, and 5 years.

Table 3 Multivariate Cox Proportional Hazards Regression Model Analysis of Independent Predictors for Overall Survival

	SE	Wald	*P*	HR	95% CI	95% CI
Age	0.0186	3.13	0.0018	1.039	0.994	1.086
ASA	0.6943	1.35	0.1768	2.49	0.662	9.367
Coronary heart disease	36.4498	−0.11	0.9114	27.137	2.197	335.164
ALT	0.0236	−1.27	0.2031	0.957	0.957	1.012
CA125	0.0019	1.14	0.2540	1.002	0.998	1.007
Pathological differentiation degree	0.3247	−3.27	0.0011	0.384	0.188	0.786
Grade	0.2707	0.61	0.5432	1.363	0.721	2.578
Lymphatic Metastasis	0.4858	1.55	0.1216	1.852	0.56	6.126
Vascular invasion	0.4783	3.25	0.0011	4.208	1.523	11.625
NLR	0.0907	1.96	0.0502	1.152	0.949	1.399
SII	0.0003	6.16	<0.0001	1.001	1.001	1.002

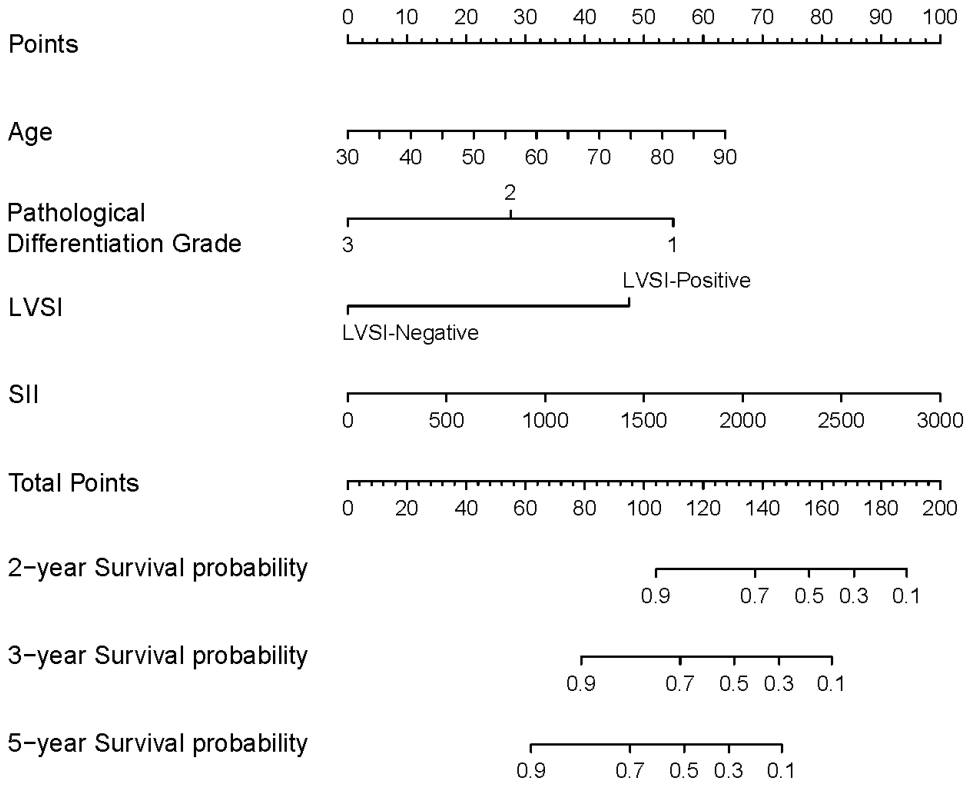

Figure 2 Nomogram of the predictive model.

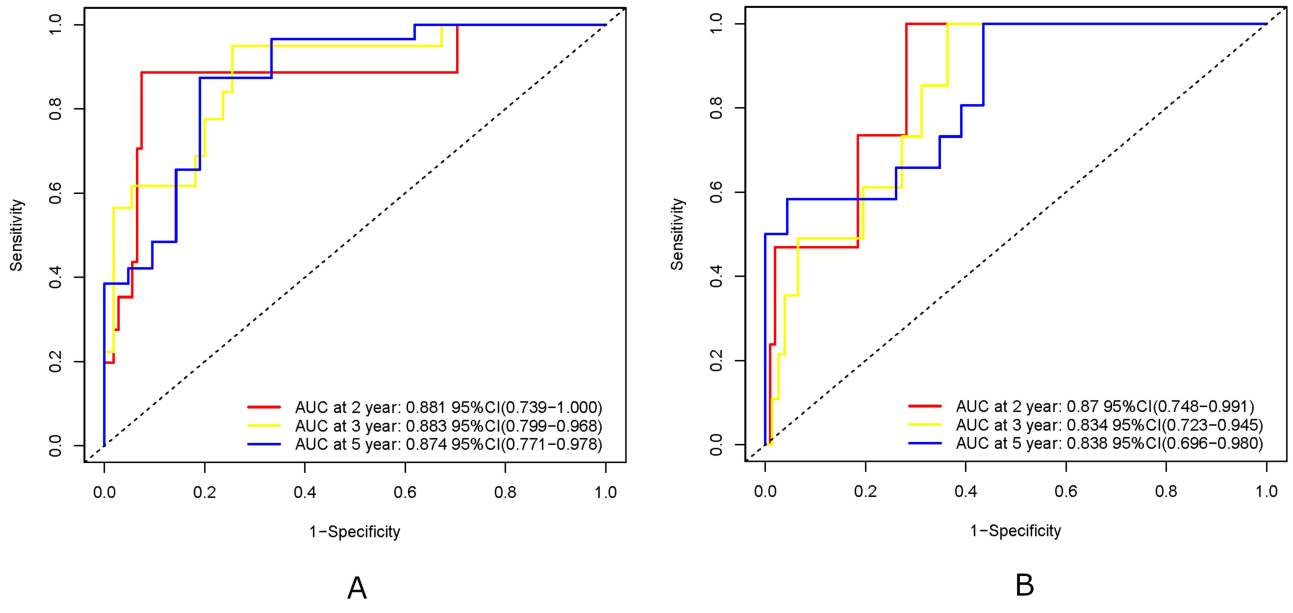

Figure 3 Receiver Operating Characteristic (ROC) Curves for Assessing the Discriminative Performance of the Prognostic Model. (**A**) ROC curve of the training set. (**B**) ROC curve of the validation set. The horizontal axis denotes "1-specificity" (ie, false positive rate), while the vertical axis corresponds to "sensitivity" (ie, true positive rate). The area under each curve (AUC) serves as an indicator of the model's capacity to differentiate between positive and negative instances, with an AUC value approaching 1 signifying superior model performance.

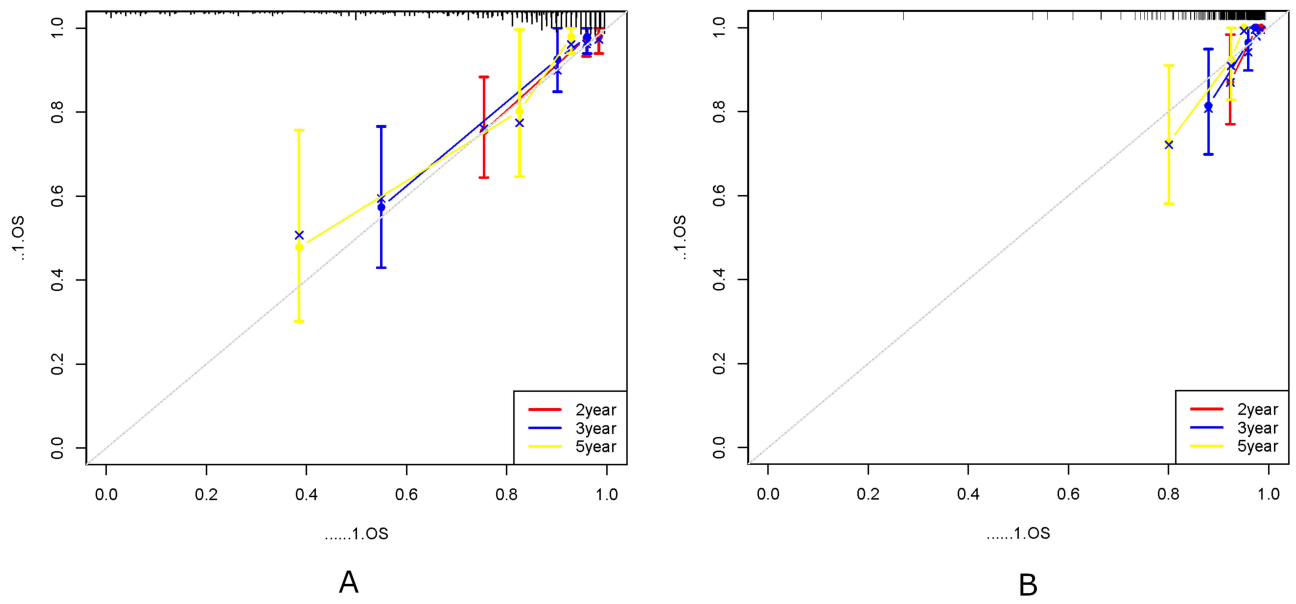

Figure 4 Calibration curves for the training and validation sets. (**A**) Calibration curve of the training set. (**B**) Calibration curve of the validation set. The horizontal axis of the graph denotes the risk probability predicted by the model, while the vertical axis corresponds to the actual proportion. The graph illustrates the discrepancies between observed values and predicted values across each group. An ideally calibrated curve should lie close to the diagonal line (gray line). The red curve represents the actual predicted probability of the model, the blue curve denotes the probability after bias correction, and the black dashed line indicates the perfect prediction under ideal circumstances. The predictive accuracy of the model can be assessed via this calibration curve; the closer the curve is to the diagonal line, the superior the model's predictive performance.

Discussion

This study developed and validated a prognostic nomogram for endometrial cancer that integrates systemic immune-inflammation index (SII) with key clinicopathological variables—age, pathological differentiation grade, and lymphovascular space invasion (LVSI). The core objective of this research is to bridge the gap between traditional empirical prognosis and precision medicine practice, providing a cost-effective, widely accessible tool for individualized risk stratification that facilitates targeted treatment decision-making, especially in healthcare settings with limited access to high-throughput molecular testing.[13] The model demonstrated robust predictive performance, with AUCs exceeding 0.83 across both training and validation cohorts, underscoring its potential as a clinically useful tool for individualized prognosis.

The incorporation of SII into the prognostic framework represents a significant advancement over traditional models that rely solely on pathological staging. SII, derived from routine complete blood counts, reflects the dynamic interplay between systemic inflammation and immune competence. Elevated SII indicates a pro-tumor inflammatory milieu characterized by increased neutrophils and platelets alongside decreased lymphocytes, which collectively promote tumor progression, angiogenesis, and immune evasion.[14,15] In our cohort, SII emerged as a strong independent predictor of survival (HR = 1.001, $P < 0.001$), consistent with growing evidence supporting its prognostic value in EC and other solid tumors.[16,17] The biological plausibility of SII lies in its ability to capture the immunosuppressive tumor microenvironment, where neutrophils and platelets facilitate metastasis through cytokine secretion and epithelial-mesenchymal transition, while lymphopenia reflects impaired anti-tumor immunity.[18,19] Importantly, SII can be obtained preoperatively, postoperatively, and during follow-up, enabling longitudinal monitoring to complement clinicopathological staging.

Age retained its prognostic significance in our model (HR = 1.039, $P = 0.002$), consistent with prior studies highlighting older age as a risk factor for poorer outcomes in EC.[20] Beyond chronological age, biological aging involves immune senescence, characterized by diminished T-cell function, reduced immune surveillance, and increased inflammatory cytokine production—a phenomenon often termed "inflammaging".[21] In EC, older patients exhibit altered tumor immune microenvironments with fewer tumor-infiltrating lymphocytes and higher regulatory T-cell infiltration, which may compromise response to therapy and facilitate recurrence.[22] Thus, age in our model may serve as a surrogate for host immune resilience and therapeutic tolerance, reinforcing the need for age-stratified management approaches—a key tenet of precision oncology that prioritizes tailored interventions to balance treatment efficacy and safety across diverse patient subgroups.

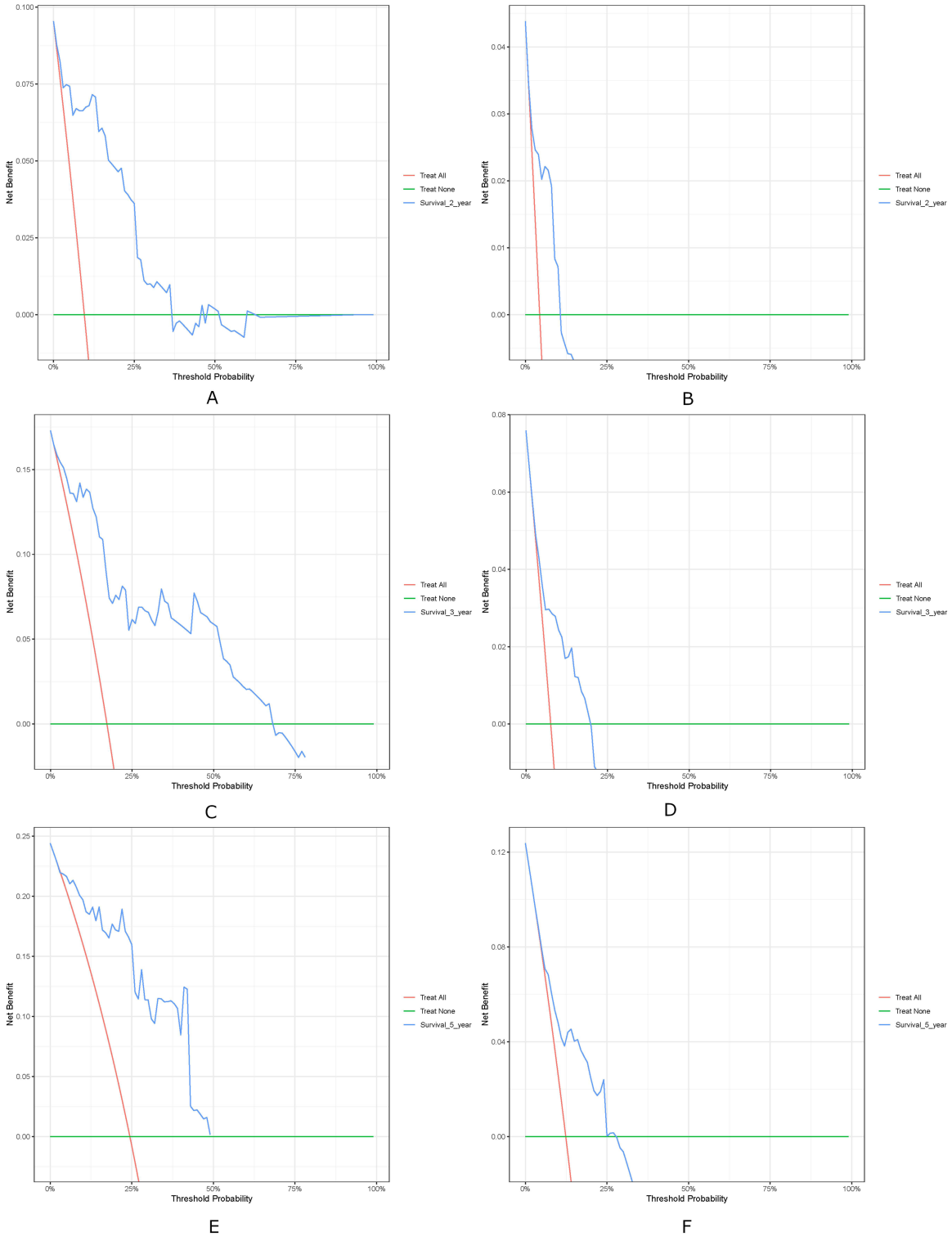

Figure 5 Decision Curve Analysis (DCA) for the Prognostic Model in the Training and Validation Cohorts. (**A** and **B**) 2-year DCA of training set and validation set. (**C** and **D**) 3-year DCA of training set and validation set. (**E** and **F**) 5-year DCA of training set and validation set. These curves assess the net benefits of the proposed model across varying high-risk thresholds. The curve denoted as "Model" corresponds to the net benefits derived from the model in question. "All" denotes the net benefits under the scenario where all patients are subjected to intervention, while "None" refers to the net benefits in the context where no patients receive intervention.

https://doi.org/10.2147/CMAR.S572098

Pathological differentiation grade was another critical determinant of prognosis, with poorly differentiated tumors (Grade 3) associated with significantly worse survival (HR = 0.384, $P = 0.001$). This aligns with established literature linking high-grade histology to aggressive tumor biology, including molecular features such as p53 mutations, microsatellite instability, and copy-number alterations.[23] The Cancer Genome Atlas (TCGA) classification further underscores the prognostic relevance of histological grade, with high-grade tumors often falling into the "copy-number high" or "p53-mutant" subgroups, which exhibit poor outcomes despite adjuvant therapy.[24] Our model leverages this well-validated parameter while augmenting it with inflammatory and host factors, thereby providing a more holistic risk assessment. Conspicuously, this integration enables the model to act as a preliminary screening tool for identifying patients at high risk of harboring adverse molecular subtypes, guiding subsequent targeted molecular testing and personalized therapeutic allocation—a strategy that aligns with the goals of pharmacogenomics in driving precision medicine.[25]

Perhaps the most potent predictor in our nomogram was lymphovascular space invasion (LVSI), which conferred a fourfold increased risk of mortality (HR = 4.208, $P = 0.001$). LVSI represents a critical step in the metastatic cascade, enabling tumor cells to enter systemic circulation and colonize distant sites.[26] Its presence is strongly correlated with lymph node metastasis, deep myometrial invasion, and higher recurrence rates.[27] Mechanistically, LVSI involves degradation of vascular basement membranes by matrix metalloproteinases and platelet-mediated protection of circulating tumor cells from immune attack.[28] The inclusion of LVSI in our model underscores the importance of local invasiveness and metastatic potential in determining prognosis, complementing systemic inflammatory and host factors. From the perspective of non-coding RNA research—an emerging frontier in EC precision oncology—LVSI and its associated metastatic potential are tightly regulated by non-coding RNAs such as microRNAs (miRNAs) and Y RNAs. For instance, circulating miRNAs have been shown to modulate EC cell invasiveness and LVSI formation,[29] while Y RNAs are increasingly recognized as key regulators of tumor metastasis and potential molecular targets.[30] Given that biomarker-informed pathways (eg, fertility-sparing decision-making) may carry clinical and legal consequences when evidence is insufficient or practice is inconsistent, these emerging ncRNA markers should be translated through analytically validated assays and guideline-concordant use to minimize unwarranted variability in care.[13,29] Future studies could explore the correlation between our model's core predictors (eg, LVSI, SII) and specific non-coding RNA signatures, thereby enhancing the molecular mechanistic basis of the nomogram and identifying novel therapeutic targets.

When compared to previously published prognostic tools, our nomogram offers several advantages. Unlike models that require specialized molecular testing or costly biomarkers, all components of our nomogram are routinely available in clinical practice.[31,32] Furthermore, by integrating inflammatory indices, our model captures the host-tumor interaction —a dimension often overlooked in traditional staging systems. Notably, integrative strategies that combine inflammation-related indices with molecular stratification are being explored across multiple malignancies; within EC, the value of our approach lies in its feasibility for repeated measurement and its potential to complement—rather than replace—molecular classifiers in individualized risk-adapted management.[13,16,17] The strong performance of our nomogram across both training and validation cohorts supports its robustness and potential for broad applicability, which is crucial for advancing precision medicine in resource-limited settings.[13] In pharmacogenomics-driven care, our model may help inform risk-adapted, guideline-concordant postoperative management, our model may help inform risk-adapted, guideline-concordant postoperative management by identifying patients who warrant intensified multidisciplinary discussion and prioritized molecular testing, while potentially sparing low-risk patients from overtreatment; prospective validation is required before treatment-selection claims can be made.[25]

Nevertheless, several limitations warrant consideration. The retrospective, single-center design may limit generalizability, and external validation in multi-institutional cohorts is needed. Inflammatory markers such as SII are non-specific and can be influenced by infections, comorbidities, or medications, which were not fully adjusted for in this analysis. Additionally, the model does not incorporate molecular classifiers (eg, POLE, MSI, p53 status), which are increasingly relevant in EC prognostication.[33] Future iterations could integrate such molecular data—including circulating miRNAs and Y RNAs—to further refine risk stratification and strengthen its relevance to precision medicine.[30] Finally, dynamic changes in SII during treatment and follow-up were not assessed; serial measurement could enhance predictive accuracy and allow for real-time risk adaptation.

Despite these limitations, our nomogram provides a pragmatic and biologically informed tool for prognostication in EC. By combining easily obtainable inflammatory and pathological variables, it facilitates individualized risk assessment and supports clinical decision-making regarding adjuvant therapy, surveillance intensity, and patient counseling. Importantly, the clinical translation of rapidly evolving therapeutic innovations—including genome editing–enabled approaches—requires robust governance, clearly defined evidence standards, and guideline development to ensure safe and equitable implementation. In the absence of such oversight, practice variability may increase, and clinical decisions that depart from evidence-based pathways can carry downstream medico-legal implications, underscoring the need for guideline-aligned governance, validation standards, and multidisciplinary oversight. Future prospective studies should validate its utility in diverse populations and explore its integration with emerging biomarkers (eg, non-coding RNAs), gene editing technologies, and imaging modalities.

Conclusion

We developed and validated a prognostic nomogram for endometrial cancer that integrates systemic immune-inflammation index with key clinicopathological factors. The model demonstrated high predictive accuracy for overall survival and offers a clinically feasible, cost-effective tool for risk stratification. By incorporating both tumor-related and host-related parameters, it provides a more comprehensive prognostic assessment than traditional staging systems. Future research should focus on external validation and integration with molecular profiling to further enhance its precision and clinical relevance.

Data Sharing Statement

The data analyzed in this study are subject to the following licenses/restrictions: The dataset originates from a single medical center and has limitations. Requests to access these datasets should be directed to Luxxbao@hotmail.com.

Ethical Approval

This study was performed in line with the principles of the Declaration of Helsinki. Approval was granted by the Institutional Review Board of Huizhou Central People's Hospital (ky112025081).

Consent to Participate

The requirement for written informed consent was waived by the Ethics Committee of Huizhou Central People's Hospital for this retrospective study, due to the use of de-identified retrospective patient data with no potential for identifying individual participants and minimal associated research risks. All patient medical records and clinical data involved in the study were strictly managed and processed in accordance with the ethical guidelines for medical research involving human subjects. Patient confidentiality was rigorously preserved throughout the study process; all personal identifying information was anonymized and de-identified prior to data collection and analysis, and the data was only used for the purpose of this research.

Acknowledgments

We thank the Extreme Analytics platform for statistical support (https://www.xsmartanalysis.com).

Author Contributions

All authors made a significant contribution to the work reported, whether that is in the conception, study design, execution, acquisition of data, analysis and interpretation, or in all these areas; took part in drafting, revising or critically reviewing the article; gave final approval of the version to be published; have agreed on the journal to which the article has been submitted; and agree to be accountable for all aspects of the work.

Funding

Guangdong Basic and Applied Basic Research Foundation (2023B1515120085).

Disclosure

The authors declare that they have no known competing financial interests or personal relationships that could have appeared to influence the work reported in this paper.

References

1. Sung H, Ferlay J, Siegel RL, et al. Global cancer statistics 2020: GLOBOCAN estimates of incidence and mortality worldwide for 36 cancers in 185 countries. *CA Cancer J Clin*. 2021;71(3):209–249. doi:10.3322/caac.21660
2. Ureyen I, Karalok A, Turkmen O, et al. Factors predicting recurrence in patients with stage IA endometrioid endometrial cancer: what is the importance of LVSI? *Arch Gynecol Obstet*. 2020;301(3):737–744. doi:10.1007/s00404-019-05418-z
3. Wright JD, Barrena Medel NI, Sehouli J, Fujiwara K, Herzog TJ. Contemporary management of endometrial cancer. *Lancet*. 2012;379 (9823):1352–1360. doi:10.1016/S0140-6736(12)60442-5
4. Greten FR, Grivennikov SI. Inflammation and cancer: triggers, mechanisms, and consequences. *Immunity*. 2019;51(1):27–41. doi:10.1016/j.immuni.2019.06.025
5. Diakos CI, Charles KA, McMillan DC, Clarke SJ. Cancer-related inflammation and treatment effectiveness. *Lancet Oncol*. 2014;15(11):e493–503. doi:10.1016/S1470-2045(14)70263-3
6. Muangto T, Maireang K, Poomtavorn Y, et al. Study on preoperative neutrophil/lymphocyte (NLR) and Platelet/Lymphocyte Ratio (PLR) as a predictive factor in endometrial cancer. *Asian Pac J Cancer Prev*. 2022;23(10):3317–3322. doi:10.31557/APJCP.2022.23.10.3317
7. Huang Y, Chen Y, Zhu Y, et al. Postoperative Systemic Immune-Inflammation Index (SII): a superior prognostic factor of endometrial cancer. *Front Surg*. 2021;8:704235. doi:10.3389/fsurg.2021.704235
8. Yan Q, Ertao Z, Zhimei Z, et al. Systemic immune-inflammation index (SII): a more promising inflammation-based prognostic marker for patients with synchronic colorectal peritoneal carcinomatosis. *J Cancer*. 2020;11(18):5264–5272. doi:10.7150/jca.46446
9. Kurklu HA, Tan TS. Systemic immune-inflammation index predicts post-MI left ventricular remodeling. *Int J Cardiovasc Imaging*. 2024;40 (5):991–1000. doi:10.1007/s10554-024-03064-4
10. Polterauer S, Zhou Q, Grimm C, et al. External validation of a nomogram predicting overall survival of patients diagnosed with endometrial cancer. *Gynecol Oncol*. 2012;125(3):526–530. doi:10.1016/j.ygyno.2012.03.030
11. Yu Z, Wei S, Zhang J, et al. Development and validation of a novel prognostic model for endometrial cancer based on clinical characteristics. *Cancer Manag Res*. 2021;13:8879–8886. doi:10.2147/CMAR.S338861
12. Riley RD, Snell KI, Ensor J, et al. Minimum sample size for developing a multivariable prediction model: PART II - binary and time-to-event outcomes. *Stat Med*. 2019;38(7):1276–1296. Erratum in: Stat Med. 2019 Dec 30;38(30):5672. doi: 10.1002/sim.8409. doi:10.1002/sim.7992
13. Gulìa C, Signore F, Gaffi M, et al. Y RNA: An overview of their role as potential biomarkers and molecular targets in human cancers. *Cancers*. 2020;12(5):1238. doi:10.3390/cancers12051238
14. Liu C, Yin Q, Wu Z, et al. Inflammation and immune escape in ovarian cancer: pathways and therapeutic opportunities. *J Inflamm Res*. 2025;18:895–909. doi:10.2147/JIR.S503479
15. Labelle M, Hynes RO. The initial hours of metastasis: the importance of cooperative host-tumor cell interactions during hematogenous dissemination. *Cancer Discov*. 2012;2(12):1091–1099. doi:10.1158/2159-8290.CD-12-0329
16. Huang Y, Gao Y, Wu Y, Lin H, Wilson JO, Crivellaro S. Prognostic value of systemic immune-inflammation index in patients with urologic cancers: a meta-analysis. *World J Urol*. 2020;38(4):897–906. doi:10.1007/s00345-019-02898-1
17. Li L, Li Y, Lu M, et al. The combination of baseline neutrophil to lymphocyte ratio and dynamic changes during treatment can better predict the survival of osteosarcoma patients. *Front Oncol*. 2023;13:1235158. doi:10.3389/fonc.2023.1235158
18. Dunn GP, Old LJ, Schreiber RD. The immunobiology of cancer immunosurveillance and immunoediting. *Immunity*. 2004;21(2):137–148. doi:10.1016/j.immuni.2004.07.017
19. Wu G, Pan B, Shi H, et al. Neutrophils' dual role in cancer: from tumor progression to immunotherapeutic potential. *Int Immunopharmacol*. 2024;140:112788. doi:10.1016/j.intimp.2024.112788
20. Shoraka M, Wang S, Carbajal-Mamani SL, Han H, Amaro B, Cardenas-Goicoechea J. Oncologic outcomes in older women with endometrial carcinoma (≥70 years). *J Obstet Gynaecol*. 2022;42(6):2127–2133. doi:10.1080/01443615.2022.2033962
21. Goronzy JJ, Weyand CM, Hu Y. Immune senescence and cardiovascular disease. *Circ Res*. 2019;124(6):920–933. doi:10.1161/CIRCRESAHA.118.314316
22. Zhang Y, Wang X, Wang J, Miao S, Chen Y, Wang L. Age-related changes in the tumor microenvironment alter anti-tumor immunity in endometrial cancer. *J Immunother Cancer*. 2022;10(6):e004685.
23. Kandoth C, Schultz N, Cherniack AD. TCGA research network. Comprehensive molecular characterization of endometrial carcinoma. *Nature*. 2013;497(7447):67–73. doi:10.1038/nature12113
24. Remmerie M, Janssens V. Targeted therapies in type II endometrial cancers: too little, but not too late. *Int J Mol Sci*. 2018;19(8):2380. doi:10.3390/ijms19082380
25. Sadee W, Wang D, Hartmann K, Toland AE. Pharmacogenomics: driving personalized medicine. *Pharmacol Rev*. 2023;75(4):789–814. doi:10.1124/pharmrev.122.000810
26. Deng L, Wang QP, Yan R, et al. The utility of measuring the apparent diffusion coefficient for peritumoral zone in assessing infiltration depth of endometrial cancer. *Cancer Imaging*. 2018;18(1):23. doi:10.1186/s40644-018-0156-6
27. Mueller JJ, Pedra Nobre S, Braxton K, et al. Incidence of pelvic lymph node metastasis using modern FIGO staging and sentinel lymph node mapping with ultrastaging in surgically staged patients with endometrioid and serous endometrial carcinoma. *Gynecol Oncol*. 2020;157 (3):619–623. doi:10.1016/j.ygyno.2020.03.025
28. Madeddu C, Sanna E, Gramignano G, et al. Correlation of leptin, proinflammatory cytokines and oxidative stress with tumor size and disease stage of endometrioid (Type I) endometrial cancer and review of the underlying mechanisms. *Cancers*. 2022;14(2):268. doi:10.3390/cancers14020268
29. Piergentili R, Gullo G, Basile G, et al. Circulating miRNAs as a tool for early diagnosis of endometrial cancer-implications for the fertility-sparing process: clinical, biological, and legal aspects. *Int J Mol Sci*. 2023;24(14):11356. doi:10.3390/ijms241411356

30. Ramaswami R, Bayer R, Galea S. Precision medicine from a public health perspective. *Annu Rev Public Health*. 2018;39(1):153–168. doi:10.1146/annurev-publhealth-040617-014158
31. Tang J, Ma W, Luo L. Establishment of the prognosis predicting signature for endometrial cancer patient. *Med Sci Monit*. 2019;25:8248–8259.
32. Shen Y, Tian Y, Ding J, et al. Unravelling the molecular landscape of endometrial cancer subtypes: insights from multiomics analysis. *Int J Surg*. 2024;110(9):5385–5395. doi:10.1097/JS9.0000000000001685
33. Kyo S, Nakayama K. Endometrial cancer as a metabolic disease with dysregulated PI3K signaling: shedding light on novel therapeutic strategies. *Int J Mol Sci*. 2020;21(17):6079. doi:10.3390/ijms21176073